

We are IntechOpen, the world's leading publisher of Open Access books Built by scientists, for scientists

4,800

Open access books available

122,000

International authors and editors

135M

Downloads

Our authors are among the

154

Countries delivered to

TOP 1%

most cited scientists

12.2%

Contributors from top 500 universities



WEB OF SCIENCE™

Selection of our books indexed in the Book Citation Index
in Web of Science™ Core Collection (BKCI)

Interested in publishing with us?
Contact book.department@intechopen.com

Numbers displayed above are based on latest data collected.
For more information visit www.intechopen.com



Kinematic Analysis of the Triangle-Star Robot with Telescopic Arm and Three Kinematics Chains as T-S Robot (3-PRP)

Ahmad Zahedi, Hadi Behzadnia,
Hassan Ghanbari and Seyed Hamed Tabatabaei

Additional information is available at the end of the chapter

<http://dx.doi.org/10.5772/64556>

Abstract

In this chapter, the limitations and weaknesses of the motion geometry and the workspace of Triangle-Star Robot {T-S (3-PRP)} are diagnosed after research and consideration of the issues at hand. In addition, they are offered in index form. To remove the problems with the abovementioned cases, at first, a robot with telescopic arms and a similar kinematics chain is rendered to give a kinematics analysis approach like Hartenberg-Denavit. Furthermore, in order to increase the workspace, Reuleaux Triangle-Star Robot {RT-S (3-PRP)} with kinematics chains 3-PRP and Circle-Star Robot{C-S (3-PRP)} with kinematics chains 3-PRP and a new improved structure are introduced.

Keywords: automation, robot, kinematics, telescopic arms, stiffness, workspace

1. Introduction

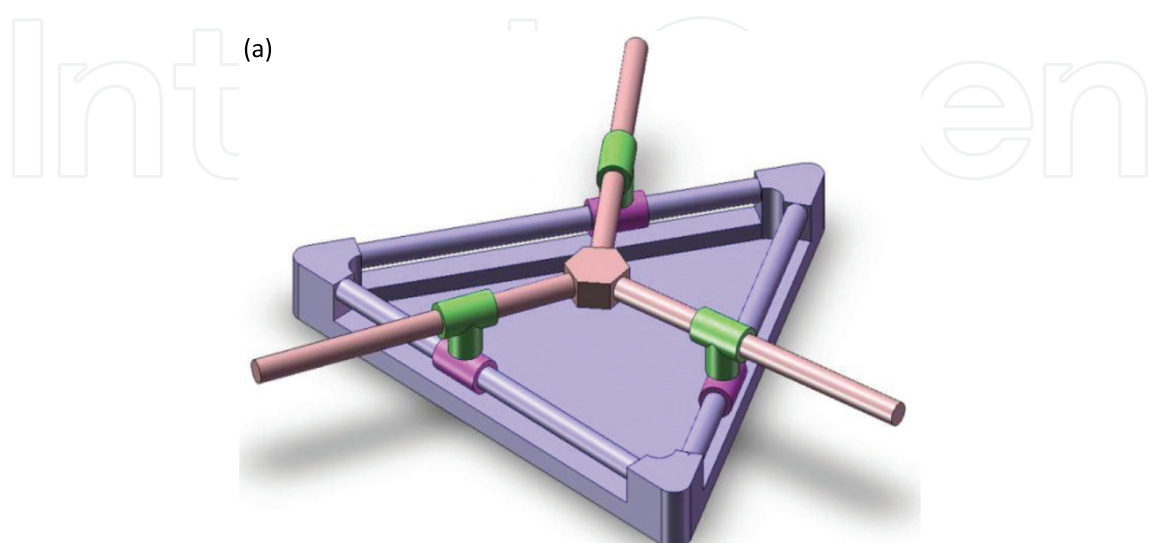
In recent decades, the use of industrial robots in the production and development of nano technological processes, industrial automation, chemically contaminated environments, medical & biological industrial, the calibration of measurement system, etc., are seriously in circulation. So the scientific research centers are conducting some research in this regard to meet customers' demands. To compete with international markets, parameters such as precision, high repeatability in production, control management, and emphasis on standards have proved to be necessary in the usage of robot in modern technology. This has caused the companies to

move toward a practical system to produce the maximum production variety at minimum time with the lowest expenses and the highest quality. Thus, the industrial automation with the help of robots replaces human force in production and in assembly lines.

Today, robots are divided into several groups: Serial robots, Parallel robots, Synthetic robots, and Mobile robots [2, 5]. Synthetic robots are to incorporate the serial and parallel manipulators by connecting them in serial. The serial connections of serial and parallel manipulators can be categorized into the following four types: Parallel-Parallel, Serial-Parallel, Parallel-Serial, and Serial-Serial [8]. Characteristics such as precision, speed, stiffness, and a workspace without singularity points have differentiated the Parallel robot from the Serial robots [4, 5]. The Parallel manipulator robots are used in making flight simulators, helicopters, machinery tools, precise robots, etc. The reverse kinematics solution of these robots as compared with the simple Serial robots and direct kinematics solution is hard with complicated equations [3, 8]. In this paper, first, the geometric attributes of the Triangle-Star Robot are offered and then based on motion geometry and robotic workspace, the limitations and weaknesses are recognized and indexically represented. In addition, to removing the abovementioned shortcomings, a new Triangle-Star Robot with telescopic arms and two new robots with improved structures are represented. Finally, the kinematics analysis of the robots similar to Denavit–Hartenberg approach is carried out.

2. Geometric characteristics of the Triangle-Star Robot

The geometric model of the Triangle-Star Robot (T-S Robot), shown in **Figure 1 (a, b)**, is composed of a $A_1 A_2 A_3$ fixed triangle and a moving star with $B_1 B_2 B_3$ arms in which the B star can move on triangle A with three kinematics chains 3-PRP.



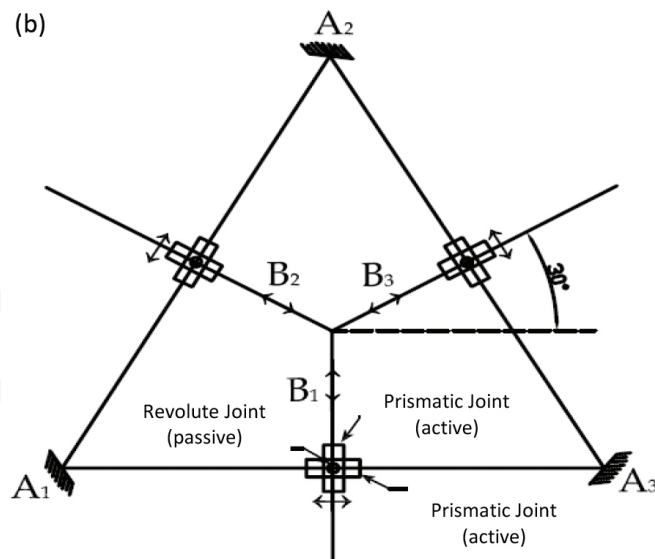


Figure 1. (a) The Triangle-Star Robot (T-S Robot) with rigid arms and (b) the geometric model of T-S Robot with rigid arms.

The motion geometry of each of the kinematics chains 3-PRP, which has been applied to T-S Robot, is achieved through relative movement of the Prismatic joint, Revolute joint, and again the Prismatic joint as shown in **Figure 2**.

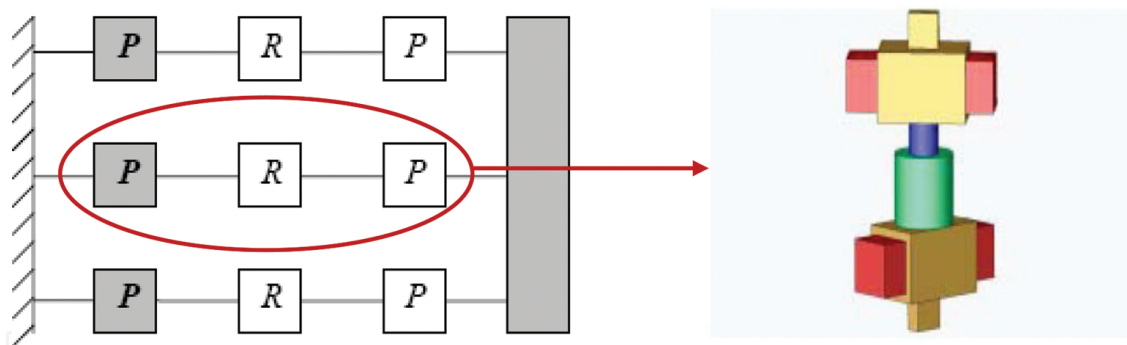


Figure 2. The motion geometry of the kinematics chains (3-PRP) for T-S Robot.

The lower active Prismatic joint movement joined to the stimulator in the direction of the angle of the triangle causes movement in the upper passive Prismatic joint connected to lower active Prismatic joint by the Revolute joint. As a result, star motion geometry, which is sited (fixed) on the upper Prismatic joints, serves as a function of the lower Prismatic movement joined to the stimulators.

3. The number of degree-of-freedom for T-S Robot

The most famous and prevalent method to calculate the degree of freedom (DOF) is using formula (1) and according **Table 1** [9].

$$F = 6(N - L - 1) + \sum_{i=1}^n f_i \quad (1)$$

N = The number of arms, L = The number of robotic joints, f_i = Indicated of DOF related i joint as shown in the above mentioned table. On the other hand, in the parallel manipulator robot, $N = 8$, $L = 9$ and f_i for $i = 1, \dots, 9$ equals 1, thus the robot's DOF is equal to 3.




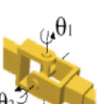

Joint	Diagram	Symbol	DOF
Revolute		R	1
Prismatic		P	1
Cylindric		C	2
Universal		T	2
Spherical		S	3

Table 1. DOF for type of joint [9].

4. The weaknesses of the motion geometry for T-S Robot

Although T-S Robot has so many advantages such as high precision, speed, stiffness, and lack of singularity in workspace, it has two main weaknesses:

1. At the time of Robotic motion, the star arms occupy a large space around the triangle
2. The abovementioned robot has a rather limited workspace

Therefore, to remove the first problem, a robot with telescopic arms, **Figure 3 (a, b)**, is introduced whose kinematics are conducted without getting involved in the whole discussion.

To remove the second problem, new robots with improved structures are introduced. The schematic design of these robots, **Figure 4 (a, b)** and their three-dimensional designs in the kinematics analysis section of each robot in **Figure 14a** and **Figure 14b** along with robot motion geometry structure are shown.

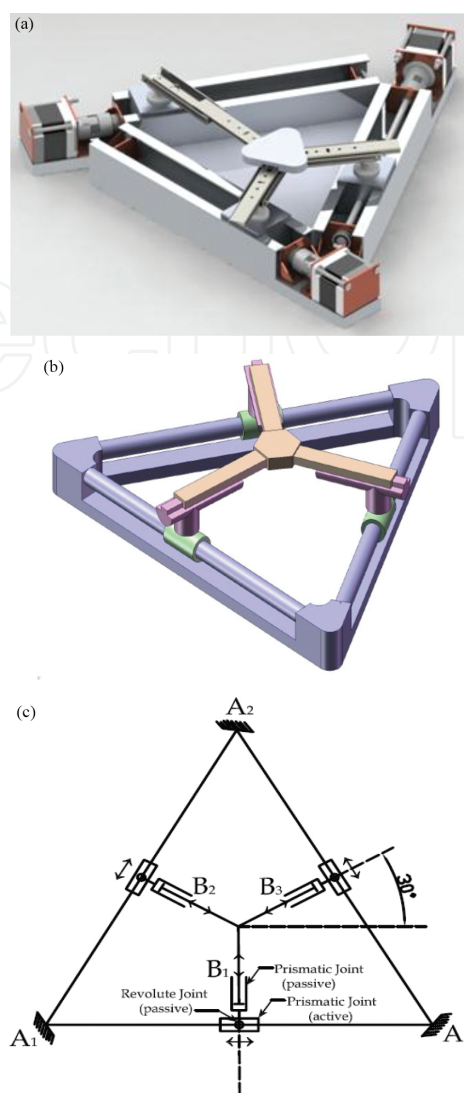
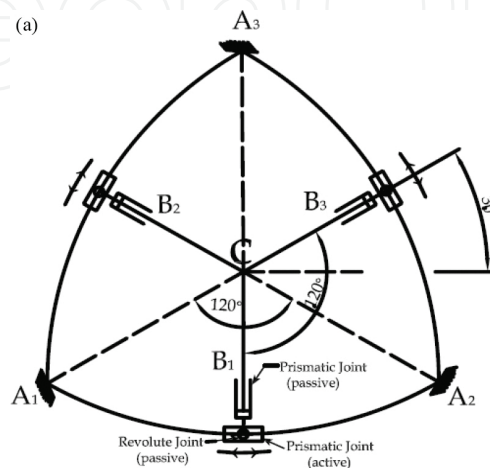


Figure 3. (a) Real model of the Triangle-Star Robot' components with telescopic arms. (b) The Triangle-Star Robot (T-S Robot) with telescopic arms. (c) The geometric model of T-S Robot with telescopic arms.



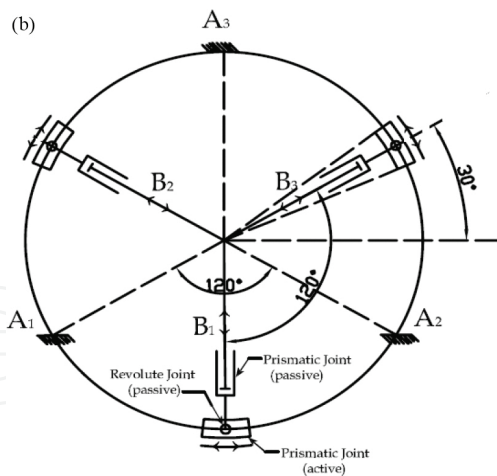


Figure 4. (a) Introduction a new geometric model as Reuleaux Triangle-Star Robot with telescopic arms. (b) Introduction of a new geometric model as Circle-Star robot with telescopic arms.

These robots are as follows:

- a. Reuleaux Triangle-Star Robot with kinematics structure {RT-S (3-PRP)}
- b. Circle-Star Robot with kinematics structure {C-S (3-PRP)}

5. Kinematic analysis of the T-S Robot

In the boundary of kinematics science, place, speed, acceleration, and all the derivations higher than local variable (in proportion to time) are examined. As defined [2, 8], the robotic kinematics is the study of the robotic movement without the consideration of the forces and torques applied to it. As a matter of fact, the examination of robotic motion geometry is regarded as an invariable coordinate frame work proportional to the intended time.

The kinematics problem includes the following sections [2, 8]:

1. Direct kinematics: local calculation and the central manipulator orientation in relation to basic frame work.
2. Reverse kinematics: if the location and central manipulator orientation are given, the calculation of all the possible joint angles involved in directing the robot toward a desired location and orientation is called reversed kinematics.

A systematic, practical approach has been represented by Denavit-Hartenberg to determine rotation and transformation between the two adjacent links in a robot [2].

In this paper, direct kinematics and reverse kinematics are examined through this approach and then position analysis, speed, input, and output acceleration are closely studied. The interesting point is that the direct kinematics of Parallel arms is as complicated as the reverse kinematics of Serial arms and the simplicity of the reverse kinematics of parallel mechanisms is as much as the simplicity of the direct kinematics of Serial arms [2, 5].

6. The extraction of Denavit-Hartenberg parameters for T-S Robot

To achieve $a_i^k, \alpha_i^k, S_i^k, \theta_i^k$ parameters, first, the position of coordinate axis according to Denavit-Hartenberg model as shown in **Figure 6 (a, b)** is determined. Then by placing these parameters in Denavit-Hartenberg matrix, which is obtained by relation (2) according to **Figure 5**. Consequently, the achieved transmitted matrixes and robotic kinematics analysis are carried out.

$$q = [q_1, q_2, q_3]^T, \quad r = [r_1, r_2, r_3]^T, \quad r = f(q) \quad (2)$$

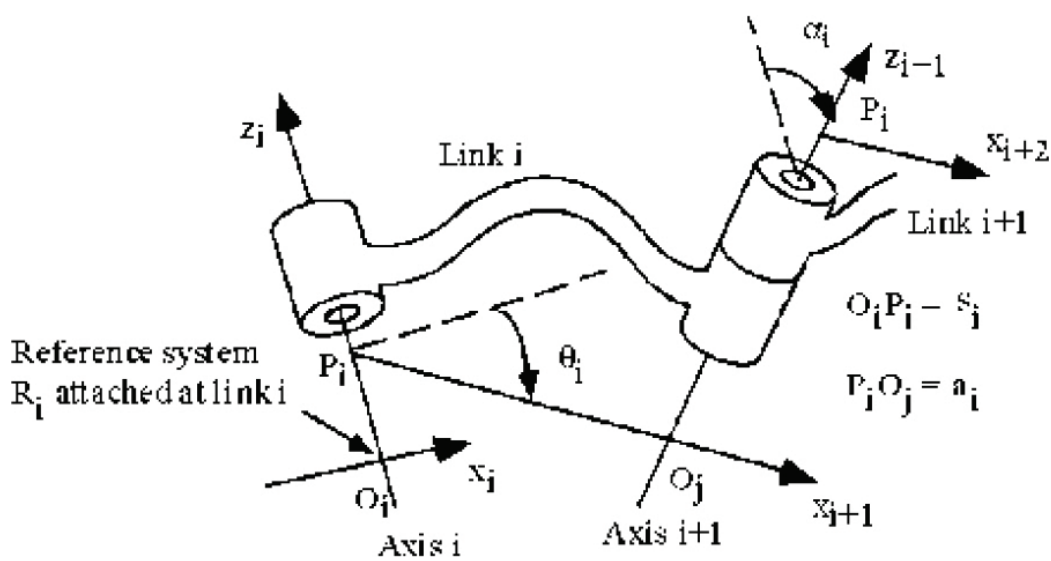
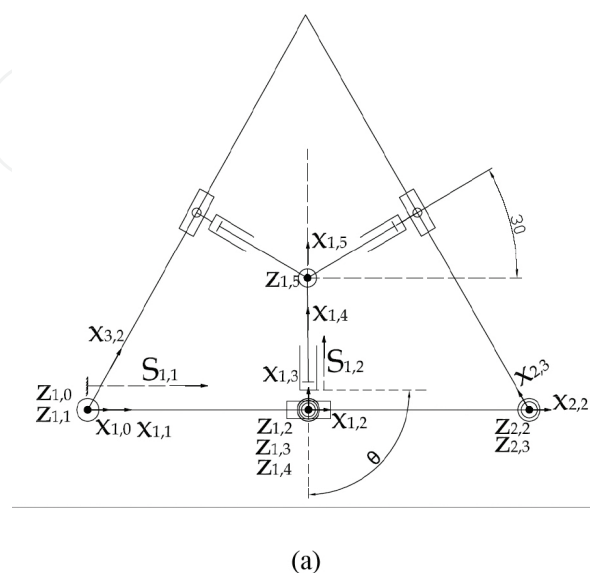


Figure 5. Kinematic chain and parameters representation of the Hartenbary–Denavit model for two adjacent links [1].



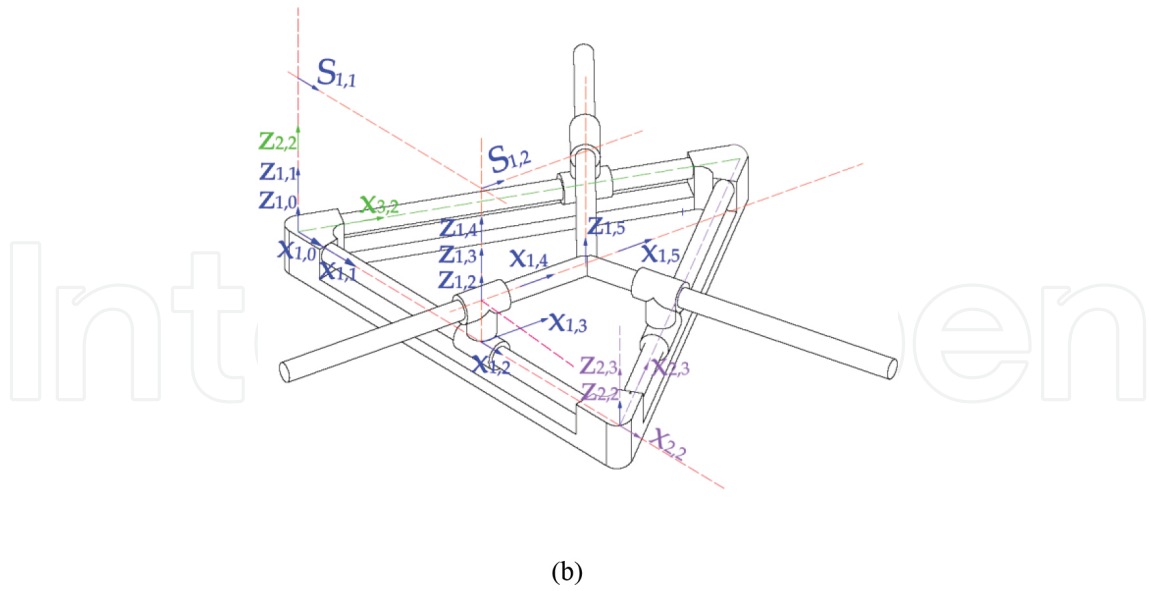


Figure 6. (a) Kinematic chain and parameters of the proposed T-S (3-PRP) robot with telescopic arms (b) Kinematic chain and parameters of the T-S robot with rigid arms.

$$H_{i,i+1}^k = \begin{bmatrix} R_{i,i+1} & P_{i,i+1} \\ [0] & 1 \end{bmatrix}, \quad i = 0,1,2, \dots (\text{joint}) \tag{3}$$

$$k = 1,2,3,4, \dots (\text{N.chain})$$

$$H_{i,i+1} = \begin{bmatrix} \cos \theta_i & -\sin \theta_i \cos \alpha_i & \sin \theta_i \sin \alpha_i & a_i \cos \theta_i \\ \sin \theta_i & \cos \theta_i \cos \alpha_i & -\cos \theta_i \sin \alpha_i & a_i \sin \theta_i \\ 0 & \sin \alpha_i & \cos \alpha_i & S_i \\ 0 & 0 & 0 & 1 \end{bmatrix} \tag{4}$$

a_i : offset distance between two adjacent joint axes, where $a_i = |p_i - o_j|$.

α_i : twist angle between two adjacent joint axes. It is the angle required to rotate the z_i axis into alignment with the z_{i+1} -axis about the positive x_{i+1} -axis according to the right-hand rule.

θ_i : joint angle between two incident normals of a joint axis. It is the angle required to rotate the x_i -axis into alignment with the x_{i+1} -axis about the positive z_i -axis according to the right-hand rule.

S_i : translational distance between two incident normals of a joint axis. $S_i = |p_i - o_i|$ is positive if the vector $p_i - o_i$ points in the positive z_i -direction; otherwise, it is negative (**Figure 6**).

To analyze the robot kinematically, first, the central manipulator point is transferred to the corner of the triangle to which the reference coordinate device is joined and through the extraction of $a_i^k, \alpha_i^k, S_i^k, \theta_i^k$ parameters, **Table 1**, related to Denavit-Hartenberg parameters, is achieved. In this case, $k = 1, 2, 3$ is the number of central manipulator point transmission,

Figure 7. These transmissions are as follows: Path 1: $C, P_{1'}, A_{1'}$ Path 2: $C, P_{3'}, A_{3'}, A_{1'}$ Path 3 : $C, P_{2'}, A_{1'}$

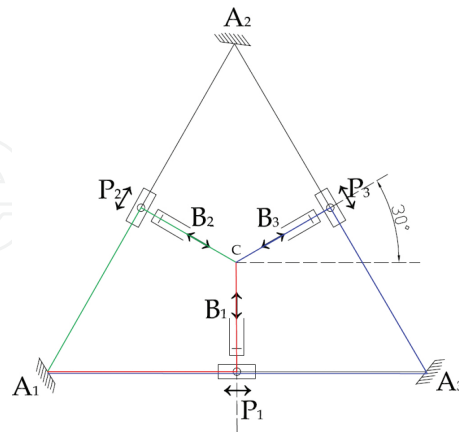


Figure 7. Transmission paths from point C to A_1 .

	Joint no.	0	1	2	3	4	5	6
Path 1	$a_{1,i}$	0	0	S_{11}	0	0	S_{13}	x
	$\alpha_{1,i}$	0	0	0	0	0	0	0
	$S_{1,i}$	0	0	0	0	b	0	0
	$\theta_{1,i}$	0	0	0	$\frac{\pi}{2} + \theta$	0	0	0
Path 2	$a_{2,i}$	e	0	S_{21}	0	0	S_{23}	x
	$\alpha_{2,i}$	0	0	0	0	0	0	0
	$S_{2,i}$	0	0	0	0	b	0	0
	$\theta_{2,i}$	0	$\frac{2\pi}{3}$	0	$\frac{\pi}{2} + \theta$	0	0	0
Path 3	$a_{3,i}$	0	0	S_{31}	0	0	S_{33}	x
	$\alpha_{3,i}$	0	0	0	0	0	0	0
	$S_{3,i}$	0	0	0	0	b	0	0
	$\theta_{3,s}$	$\frac{\pi}{3}$	0	0	$-\frac{\pi}{2} - \theta$	0	0	0

Table 2. Kinematics parameters of T-S robot.

In the above indexes, the first shows the number of the direction, and the second shows the number of the parameter. To avoid making mistakes, the number of direction indexes (first index) is shown to the power of k .

By placing **Table 2** parameters, in matrix 2, the amount of $H_{i,i+1}^k$ matrix is achieved in which, $i = 1, 2, 3, 4$ is the number of coordinate systems joined to the links and $k = 1, 2, 3$ is the number of the central manipulator reference point directions joined to C point. The speed-acceleration points are obtained through placing the position analysis matrixes two by two in an equal way.

7. Direct kinematics for T-S robot

For the direct kinematics analysis, point o , located in the origin of the coordinate of A_1 , reference system is regarded as the primary point and o' , point in the origin of the coordinate joined to the center of C point, is considered to be the final point.

The number of unknown parameters in each path is two. As a result, the total number of unknown parameter for each path is 6, but since the number of degree of freedom for each kinematics chains 3-PRP equals 9, the number of each path of the unknown parameters is 3, that is, the three parameters are related to other parameters that are geometrically obtained. In this case, the robotic degree of freedom is 3. If S_{11} , S_{21} , S_{31} parameters are considered to be the inputs, the unknown parameters will be S_{13} , S_{23} , S_{33} and θ_{11} , θ_{21} , θ_{31} .

What is stated is for the simplification and avoidance of mistakes in the number of direction index to the power of k . Therefore, to obtain the unknown parameters, final point transformation matrix o' is obtained in proportion to the primary point o and then relation (5, 11) is used.

$$[P]_i = H_{o,o'}^k [P]_{i+1} \quad (5)$$

$$H_{o,o'}^k = H_{0,1}^K \times H_{1,2}^K \times H_{2,3}^K \times H_{3,4}^K \dots H_{i,i+1}^K \quad (6)$$

$$H_{o,o'}^1 = H_{o,o'}^1 = H_{o,o'}^3 \quad (7)$$

$$[P_{o'}]_{(O)(for.path1)} = [P_{o'}]_{(O)(for.path2)} = [P_{o'}]_{(O)(for.path3)} \quad (8)$$

$$\begin{aligned} [P]_i &= [H_{i,i+1}^k] \cdot [P]_{i+1} \\ [P]_i &= [x_i; y_i; z_i; 1] \end{aligned} \quad (9)$$

In the above relation, $[P]_i$ is the position in relation to coordinate axes joined to member i , and $[P]_{i+1}$ is the position in relation to coordinate axes joined to member $i + 1$. The robot has three kinematics chains, and three different transformation matrixes are achieved. In this way, the three matrixes should be equalized according to relation (5). The unknown parameters are obtained through the solution of these equations.

Point o' coordinate (P_3 origin of coordinate) located in the center of the star in P_2 coordinate is as follows. Point o' coordinates in P_0 coordinate is as follows:

$$[P_{O'}]_{(2)} = [P_i] = [x_O; y_O; z_O; 1]_{(2)} = [0; 0; S_2^k; 1]_{(2)} \quad (10)$$

$$[P_{O'}]_{(0)} = \begin{bmatrix} x_{O'} \\ y_{O'} \\ z_{O'} \\ 1 \end{bmatrix}_{(0)} = \begin{bmatrix} x_{O'} \\ y_{O'} \\ z_{O'} \\ 1 \end{bmatrix}_{(0)} = [H_{0,1}^K] \times [H_{1,2}^K] \times [H_{2,3}^K] \times \begin{bmatrix} 0 \\ 0 \\ S_2^K \\ 1 \end{bmatrix}_{(2)} \quad (11)$$

$$H_{0,O'}^1 = \begin{bmatrix} -\sin\theta & -\cos\theta & 0 & -\sin\theta \times x - \sin\theta \times S_3^1 + S_1^1 \\ \cos\theta & -\sin\theta & 0 & \cos\theta \times x + \cos\theta \times S_3^1 \\ 0 & 0 & 1 & B \\ 0 & 0 & 0 & 1 \end{bmatrix} \quad (12a)$$

$$H_{O',O'}^2 = \begin{bmatrix} \wp & -\Re & 0 & \wp \times x + \wp \times S_3^2 - 0.5 \times S_1^2 + e \\ \Re & \wp & 0 & \Re \times x + \Re \times S_3^2 + 0.866 \times S_1^2 \\ 0 & 0 & 1 & b \\ 0 & 0 & 0 & 1 \end{bmatrix}$$

$$\Re = -0.866\sin\theta - 0.5\cos\theta$$

$$\wp = 0.5\sin\theta - 0.866\cos\theta, \quad (12b)$$

$$H_{O',O'}^2 = \begin{bmatrix} \wp' & -\Re' & 0 & \wp' \times x + \wp' \times S_3^3 + 0.5 \times S_1^3 \\ \Re' & \wp' & 0 & \Re' \times x + \Re' \times S_3^3 + 0.866 \times S_1^3 \\ 0 & 0 & 1 & b \\ 0 & 0 & 0 & 1 \end{bmatrix}$$

$$\wp' = -0.5\sin\theta + 0.866\cos\theta$$

$$\Re' = -0.866\sin\theta - 0.5\cos\theta$$

$$path(1): \begin{bmatrix} x_{O'} \\ y_{O'} \\ z_{O'} \\ 1 \end{bmatrix}_{(0)} = \begin{bmatrix} -x \times \sin\theta - S_3^1 \times \sin\theta + S_1^1 \\ x \times \cos\theta + S_3^1 \times \cos\theta \\ b \\ 1 \end{bmatrix} \quad (13ab)$$

$$path(2): \begin{bmatrix} x_{O'} \\ y_{O'} \\ z_{O'} \\ 1 \end{bmatrix}_{(0)} = \begin{bmatrix} \wp \times x + \wp \times S_3^2 - 0.5 \times S_1^2 + e \\ \Re \times x + \Re \times S_3^2 + 0.866 \times S_1^2 \\ b \\ 1 \end{bmatrix}$$

$$path.(3): \begin{bmatrix} x_{O'} \\ y_{O'} \\ z_{O'} \\ 1 \end{bmatrix}_{(0)} = \begin{bmatrix} \wp' \times x + \wp' \times S_3^3 + 0.5 \times S_1^3 \\ \mathfrak{R}' \times x + \mathfrak{R}' \times S_3^3 + 0.866 \times S_1^3 \\ b \\ 1 \end{bmatrix} \quad (13c)$$

8. The motion geometry of T-S Robot

$$\phi_3 + \phi_5 = 180, \phi_5 = \frac{\pi}{2} + \theta_3, \phi_3 = \frac{\pi}{2} + \theta_2 \Rightarrow \theta_2 = -\theta_3, \phi_1 + \phi_2 = 180, \phi_1 = \frac{\pi}{2} + \theta_1, \phi_2 = \frac{\pi}{2} - \theta_2 \Rightarrow \theta_1 = \theta_2$$

$$\theta_1^1, \theta_1^2, \theta_1^3 = \theta, \sin \theta = \frac{2t}{1+t^2}, \cos \theta = \frac{1-t^2}{1+t^2}, t = \tan \frac{\theta}{2}$$

From the motion geometry of the T-S robot and then relations (5,13), the motion equation are achieved.

$$-0.75x \times \sin \theta - S_3^1 \times \sin \theta + S_1^1 + 0.866x \times \cos \theta - 0.5S_3^2 \times \sin \theta + 0.866S_3^2 \cos \theta + 0.5S_1^2 - e = 0 \quad (14a)$$

$$0.75x \times \cos \theta + S_3^1 \times \cos \theta + 0.866x \times \sin \theta + 0.866S_3^2 \times \sin \theta + 0.5S_3^2 \cos \theta + 0.866S_1^2 = 0 \quad (14b)$$

$$-0.75x \times \sin \theta - S_3^1 \times \sin \theta + S_1^1 - 0.866x \times \cos \theta - 0.5S_3^3 \times \sin \theta - 0.866S_3^3 \cos \theta - 0.5S_1^3 = 0 \quad (14c)$$

$$0.75x \times \cos \theta + S_3^1 \times \cos \theta - 0.866x \times \sin \theta - 0.866S_3^3 \times \sin \theta + 0.5S_3^3 \cos \theta - 0.866S_1^3 = 0 \quad (14d)$$

$$-1.7x \times \cos \theta + 0.5S_3^2 \times \sin \theta - 0.866S_3^2 \times \cos \theta - 0.5S_1^2 - 0.5S_3^3 \sin \theta - 0.866S_3^3 \cos \theta - 0.5S_1^3 = 0 \quad (14e)$$

$$-1.7x \times \sin \theta - 0.866S_3^2 \times \sin \theta - 0.5S_3^2 \times \cos \theta + 0.866S_1^2 - 0.866S_3^3 \sin \theta + 0.5S_3^3 \cos \theta - 0.866S_1^3 = 0 \quad (14f)$$

9. Case analysis

If we consider the fixed angle of the triangle $A_1A_2A_3$ in **Figure 8**, $e = 1000$ mm, $b = 100$ mm and each of the S_{11} , S_{21} , S_{31} inputs are applied to the direction of the triangle, then **Figure 9 (a, b)** are obtained.

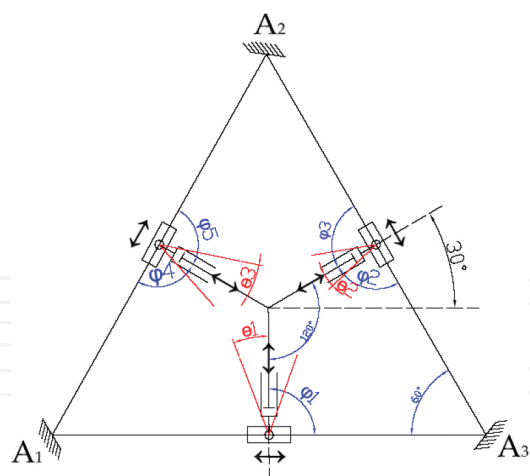
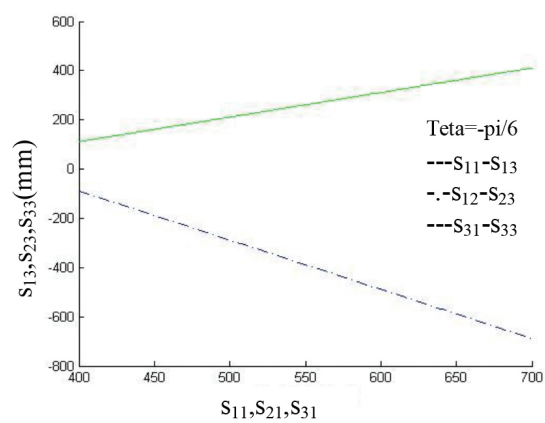
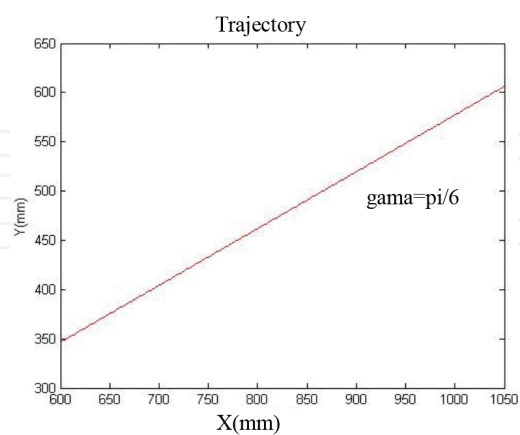


Figure 8. Geometric relation between triangle and star sides.



(a)



(b)

Figure 9. (a) Variation S_{13} , S_{23} , S_{33} (output) versus actuator S_{11} , S_{21} , S_{31} (input) and (b) X-Y plots of the trajectory of the motion point c.

10. Inverse kinematics for T-S Robot

The representation of the location and orientation of the robotic final manipulator can lead to the estimation of all the possible joint collections, which are used to transfer the robot and to obtain the assumed orientation. This process is called kinematics reverse estimation [2]. Therefore, in the reverse kinematics analysis, we have access to the coordinate components of the central point of the moving star (point C located in the reference system O') which are relative to the primary reference system and which are the goal for obtaining the unknown parameters $S_{11}, S_{21}, S_{31}, (S_1^1, S_1^2, S_1^3)$. The independent linear equations are obtained through equalizing the transformative matrixes related to the central point of the moving star.

Solving these equations in which the inputs are $\theta_1^1, \theta_1^2, \theta_1^3 = \theta$ and $S_{13}, S_{23}, S_{33} (S_3^1, S_3^2, S_3^3)$, then $S_{11}, S_{21}, S_{31} (S_1^1, S_1^2, S_1^3)$ are obtained.

$$-X \times \sin\theta - \sin\theta \times S_3^1 + S_1^1 - q_x = 0 \quad (15a)$$

$$X \times \cos\theta + \cos\theta \times S_3^1 - q_y = 0 \quad (15b)$$

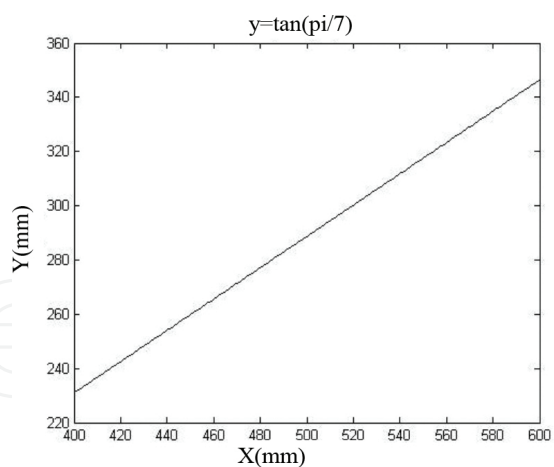
$$0.5X \times \sin\theta - 0.866X \times \cos\theta + 0.5S_3^2 \times \sin\theta - 0.866S_3^2 \times \cos\theta - 0.5S_2^1 + e - q_x = 0 \quad (15c)$$

$$-0.866X \times \sin\theta - 0.5X \times \cos\theta - 0.866S_3^2 \times \sin\theta - 0.5S_3^2 \times \cos\theta + 0.866S_2^1 - q_y = 0 \quad (15d)$$

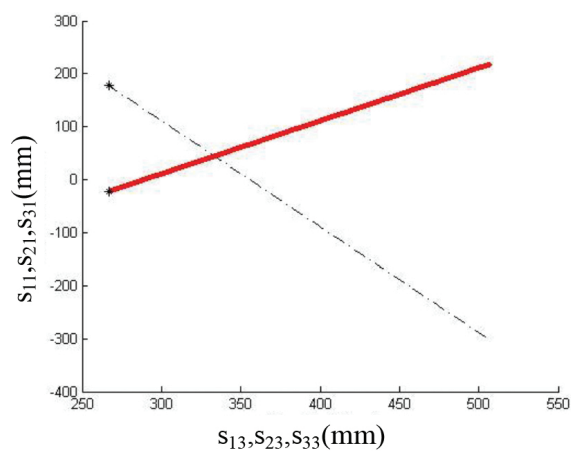
$$-0.5X \times \sin\theta + 0.866X \times \cos\theta - 0.5S_3^3 \times \sin\theta + 0.866S_3^3 \times \cos\theta + 0.5S_1^3 - q_x = 0 \quad (15e)$$

$$-0.866X \times \sin\theta - 0.5X \times \cos\theta - 0.866S_3^3 \times \sin\theta - 0.5S_3^3 \times \cos\theta + 0.5S_1^3 - q_y = 0 \quad (15f)$$

To conduct the reverse kinematics analysis, we should assume two directions: (1) linear, (2) circular, in which the center of the star (point located in O' reference system) goes through the two mentioned directions as shown in **Figure 10 (a)** and **Figure 11 (a, e)**. The outcome is respectively represented in **Figure 10 (b)** and **Figure 11 (b, c, d, e)**.

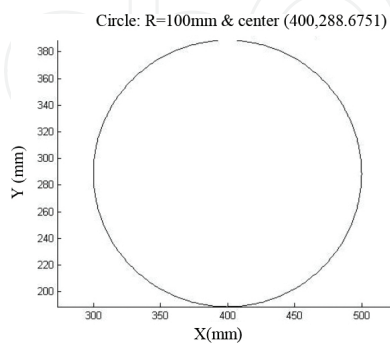


(a)

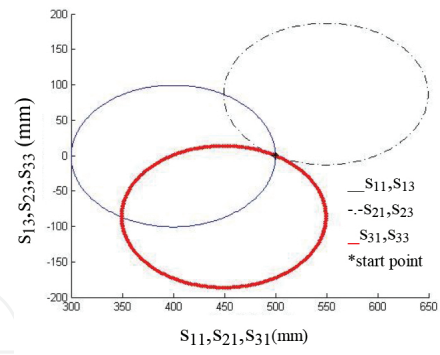


(b)

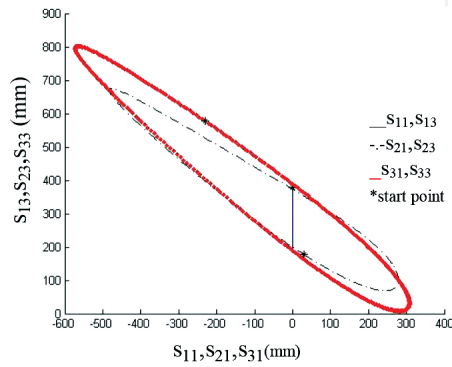
Figure 10. (a) X-Y plots of the path of the motion point c and (b) variation S_{11} , S_{21} , S_{31} (output) versus S_{13} , S_{23} , S_{33} S_{13} , S_{23} , S_{33} (mm).



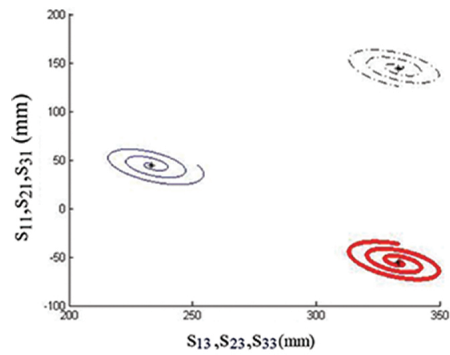
(a)



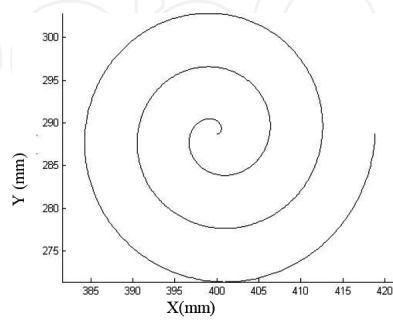
(b)



(c)



(d)



(e)

Figure 11. (a, e) X-Y plots of the path of the motion point c ; (b, d) variation S_{11}, S_{21}, S_{31} (outputs) versus S_{13}, S_{23}, S_{33} for $\theta = 0$; (c) variation S_{11}, S_{21}, S_{31} (outputs) versus S_{13}, S_{23}, S_{33} (inputs) for $\theta = \pi/6$.

11. Workspace analysis

The existence or nonexistence of the kinematics solution determines the robotic workspace. The lack of solution means that the robot is not able to obtain optimal orientation because it is located out of the workspace. These conditions are called robotic singularity states. Almost all the robots have singularity points in either the border of their workspace or in their workspace. The singularity point in the border of workspace denotes a state that occurs when the arm is fully stretched or folded on itself when the final manipulator is almost or precisely located in the border of the workspace.

On the other hand, the singularity states in the workspace signify the conditions that occur in the mechanism workspace or in general when two or some joint axes are located in one direction. When the robot is located in the singularity position, it loses all or some of its degrees of freedom in the deicardean space. It is obvious that this process is done in the border of the robotic workspace. The examination of the T-S(3-PRP) robotic workspace has shown that it has no singularity in its workspace; the robotic workspace is presented in **Figure 12** (**Figure 13**).

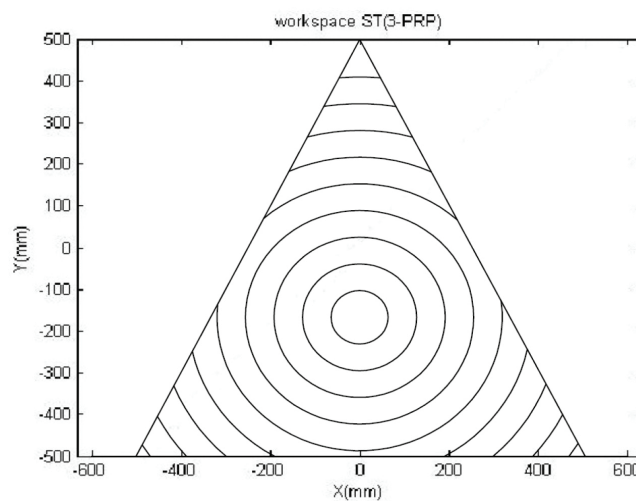


Figure 12. X-Y plots of the Achievable workspace of the T-S robot.

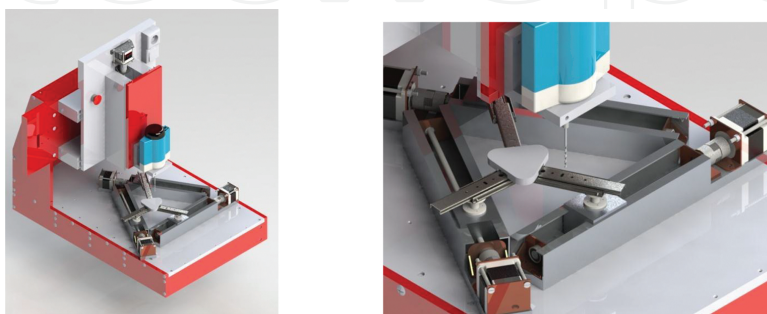


Figure 13. T-S Robot as milling machine' table.

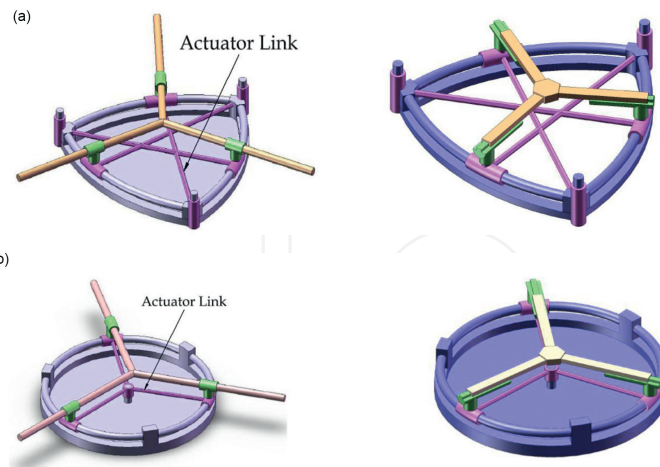


Figure 14. Introduction a new geometric model as (a) Reuleaux Triangle –Star Robot with telescopic and (b) arms Circle-Star robot with telescopic arms.

12. Conclusion

Features such as precision, speed, stiffness, and workspace with singularity point distinguish the parallel robots from the Serial robots. But the weak points of these robots compared with Serial robot are the move limited workspace. In this paper, first, the limitations and weaknesses of the Triangle-Star Robot {T-S 3(PRP)} were recognized. To remove these disadvantages, a robot with telescopic arms were presented and its kinematics analysis done through Hartenberg–Denavit instruction. In addition, there is no disturbance in the totality of the discussion.

Afterwards, to increase the workspace,

- a. Reuleaux Triangle-Star Robot with the kinematics structure {RT-S 3(PRP)}
- b. Circle-Star Robot with kinematics structure{C-S 3(PRP)} are introduced and kinematically analyzed.

Author details

Ahmad Zahedi¹, Hadi Behzadnia^{2*}, Hassan Ghanbari¹ and Seyed Hamed Tabatabaei³

*Address all correspondence to: mashaykhan@yahoo.com

1 Islamic Azad University, Firoozkooh Campus, Firoozkooh, Iran

2 Machinery Unit, The Ministry of Roads and Urban Development (MRUD), Iran

3 Islamic Azad University, South Tehran Campus, Tehran, Iran

References

- [1] Ibarreche JI, Altuzarra O, Petuya V, Hernandez A, Pinto C. Structural Synthesis of the families of parallel manipulators with 3 degrees of freedom. *Romansy 19-Robot Design, Dynamics and Control*. 2013;544: 35-42. DOI: 10.1007/978-3-7091-1379-0_5.
- [2] Chennakesava-Reddy A. Difference between Denavit - Hartenberg (D-H) Classical and Modified Conventions for Forward Kinematics of Robotics with case study, International Conference on Advanced Materials and manufacturing Technologies (AMMT); 18-20 December 2014; JNTUH College of Engineering Hyderabad. 2014. P. 267-286.
- [3] Alexander Yu, A. Bonev I, Zsombor-Murray P. Geometric Approach to the Accuracy Analysis of a Class of 3-DOF Planar Parallel Robots. *Mechanism And Machine Theory*. 2007; 43: 364-375. DOI: 10.1016/j.mechmachtheory.2007.03.002
- [4] Pandilov Z, Dukovski V. Comparison of the characteristics between serial and parallel Robots. *ACTA TEHNICA CORVINIENSIS – Bulletin of Engineering Tome VII*. 2014; 5: 143-160. DOI: 10.3311/pp.ch.2014-5.01
- [5] Lovasz E-CH, Grigorescu S, Mărgineanu D, Pop C, Gruescu C, Maniu I. Kinematics of the planar parallel Manipulator using Geared Linkages with linear Actuation as kinematic Chains 3-R(RPRGR)RR. The 14th IFToMM World Congress; 25-30 October 2015; Taipei, Taiwan; 2015. P. 1-6
- [6] Pandilov Z, V. Dukovski V. Several open problems in parallel robotics. *ACTA TECHNICA CORVINIENSIS-Bulletin of Engineering, Tome IV*. 2011; 3:77-84. DOI: 10.3311/pp.ch.2011-3.01
- [7] Chablat D, Staicu S. KINEMATICS OF A 3-PRP PLANAR PARALLEL ROBOT. *U.P.B. Sci. Bull., Series D*. 2009; 71:1-15. DOI: 0904/0904.0058
- [8] Chablat D, Wenger P. Self Motions of a Special 3-RPR Planar Parallel Robot. *Advances in Robot Kinematics*. 2006; 1: 221 – 228. DOI: 10.1177/0278364908092466
- [9] Haijun Su, Peter Dietmaier, J. M. McCarthy " Trajectory Planning for Constrained Parallel Manipulators "Robotics and Automation Laboratory, UCI, August 1, 2002

